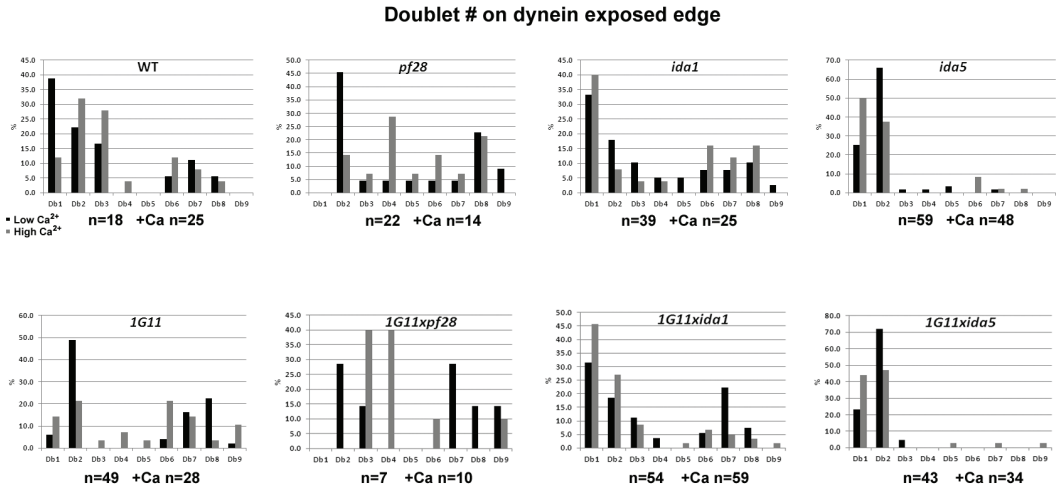

Supplemental Figure S1. **Doublet number 1 and 2 are predominately found on the dynein exposed edge.** Distributions of the doublet present at the dynein-exposed edge of the active area following induction of microtubule sliding in low (black bars) or high (grey bars) calcium concentrations. Data was collected from two independent trials and the number of transverse sections counted for each strain in low (n) or high (+Ca n) calcium buffers is listed below each table. The identity of the outer doublet on the dynein exposed edge was determined according to the criteria of Hoops and Witman (Hoops and Witman, 1983). The key identifying factor was the lack of an outer dynein arm on doublet one, the unusual cross-bridge between doublets one and two, and the beak structures in the B-tubule of doublets one, five and six. For mutants lacking the outer dyneins arms (*pf28* and *1G11xpf28*), only the cross-bridge and beak structures were used for doublet number identification.

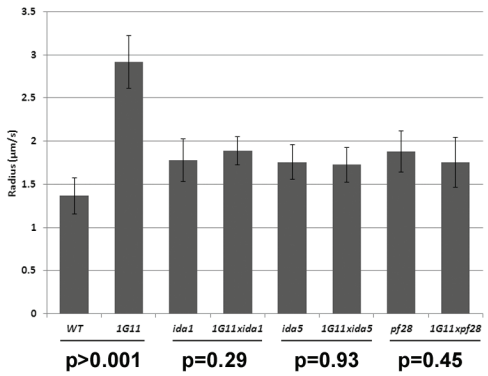

Supplemental Figure S2. **Dynein double mutants have recovered waveform curvature compared to C1d single mutant.** A graph of the average radius of the curve generated by the principal bend of the recovery stroke for each strain. The broad curve generated by *1G11* flagella is statistically different from the narrow curve generated by WT flagella. In contrast, the dynein arm double mutant flagella generate more narrow curves that are not statistically different from the corresponding single dynein mutant. ImageJ was used to measure the radius of the principal bend of the recovery stroke. The displayed radii are the average of 10 cells and the error bars represent standard deviation. P-values for each set of strains were calculated using the Student's t-test in Excel.